Noise-induced dynamical regimes in a system of globally coupled excitable units

Vladimir V. Klinshov[1], Sergey Yu. Kirillov[1], Vladimir I. Nekorkin[1], Matthias Wolfrum[2]

[1] Institute of Applied Physics Russian Academy of Sciences Ulyanova Street 46 603950 Nizhny Novgorod Russia E-Mail: vladimir.klinshov@gmail.com skirillov@ipfran.ru vnekorkin@ipfran.ru	[2] Weierstrass Institute Mohrenstr. 39 10117 Berlin Germany E-Mail: matthias.wolfrum@wias-berlin.de

Noise-induced dynamical regimes in a system of globally coupled excitable units

Vladimir V. Klinshov, Sergey Yu. Kirillov, Vladimir I. Nekorkin, Matthias Wolfrum

ABSTRACT. We study the interplay of global attractive coupling and individual noise in a system of identical active rotators in the excitable regime. Performing a numerical bifurcation analysis of the nonlocal nonlinear Fokker-Planck equation for the thermodynamic limit, we identify a complex bifurcation scenario with regions of different dynamical regimes, including collective oscillations and coexistence of states with different levels of activity. In systems of finite size this leads to additional dynamical features, such as collective excitability of different types, noise-induced switching and bursting. Moreover, we show how characteristic quantities such as macroscopic and microscopic variability of inter spike intervals can depend in a non-monotonous way on the noise level.

The concept of excitability, introduced by Wiener and Rosenblueth [28] in 1946 provided an extremely successful framework for understanding a large variety of real-life systems. Originally developed for biological systems, ranging from cardiac tissue to functionalities of organisms or behavioral aspects of animals it has also been translated to other fields e.g. gene regulatory networks, chemical reactions, laser systems, semiconductors and, finally, it has become one of the key principles in theoretical neuroscience. For a single excitable unit the influence of noise is known to induce irregular oscillations , which for a certain intermediate level of noise become most regular (coherence resonance). Here, we study how in a large system of excitable units this individual incoherent noise-induced spiking can be synchronized by an attractive global coupling. We observe, how for different noise levels qualitatively different dynamical regimes can appear and how microscopic and collective order can be both induced and dissolved by the noise.

1. INTRODUCTION

The understanding of dynamical systems under the influence of noise is an important question in nonlinear science [1]. Of particular interest are cases where the noise has a constructive influence on the dynamical behavior or some characteristic quantities depend in a non-monotonic way on the noise level. A classical example is the coherence resonance phenomenon [20], where the noise-induced oscillations of an excitable system become most coherent at a certain intermediate noise level. A similar effect has also been shown in the context of stochastic resonance where a bistable noisy system with periodic forcing becomes effectively synchronized in a region of optimally selected noise intensities [15]. The behavior of a single excitable unit under the influence of noise has been studied extensively since then [14] and also for spatially extended systems of coupled excitable units a huge variety of self organized dynamics has been shown, ranging from simple propagating pulses or waves to more complicated structures such as e.g spiral waves or exotic phenomena like coherence resonance chimeras [22].

Having in mind that for globally coupled oscillator systems the balance of disorder, either caused by individual noise or inhomogeneous frequencies, with attractive coupling typically leads to partial synchronization [11, 19], it is natural to investigate the synchronization behavior of noise-induced oscillations in a system of excitable units driven by individual noise and coupled by a global attractive coupling. However, the classical scenario of synchronization can not be easily transferred to this situation since the noise-induced oscillations do not have a definite frequency and the attractive coupling may lead both to synchrony of the oscillations as also to a mutual stabilization in the quiescent state at the stable fixed point of the excitable units.

In 1986 Shinomoto and Kuramoto [23] introduced a system of excitable active rotators with global coupling of Kuramoto type. Remarkably, they started their study on synchronizing a system of coherence resonance oscillators even before coherence resonance itself has been described in [20]. In [21] they extended their results and presented a bifurcation scenario for the Fokker-Planck equation where different collective dynamical regimes are organized by the interplay of several codimension two bifurcations. This bifurcation scenario was later recovered by means of Gaussian approximation [30] and similar scenarios have been found also for different types of systems, such as the forced Kuramoto system [3, 2], or coupled inhomogeneous populations of active rotators, both without [12] and with noise [6, 7], or pulse coupled inhomogeneous populations of active rotators [16]. Moreover, Lafuerza e.a. [12] pointed out that the onset of the collective oscillations may also depend on the type of frequency distribution. Note that for systems without noise and Lorenzian frequency distributions the Ott-Antonsen approach allows a bifurcation analysis in the framework of three ODEs [17, 18], for which some of the bifurcations can be found even analytically. For some of the dynamical regimes found in the Fokker-Planck equation, also the stochastic properties of noisy trajectories of finite size systems have been investigated. In particular, the regime of irregular collective spiking (also sometimes called "collective firing") has been studied. It is characterized by peaks in the mean field evoked by coincident excitations of many units, which can occur at sufficiently strong coupling. It has been shown that this phenomenon can be induced not only by noise, but also by inhomogeneity of the units or disorder in the coupling network [25, 26]. In [27], it has been even demonstrated that one can observe a "system size coherence resonance" for such collective excitations, i.e. they show a maximal coherence at some intermediate system
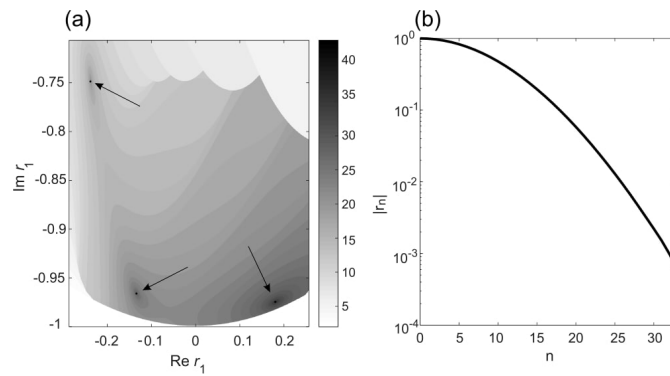
FIGURE 1. (a) Number N of iterates with $|r_n| < 1$ for $n < N$ starting with given $r_1 \in \mathbb{C}$. Sharp peaks (see arrows) correspond to series converging to equilibrium states. (b) Decay of absolute values $|r_n|$ of the order parameter versus n for a converging series with $r_1 = 0.182 - 0.975i$ corresponding to the right-bottom peak in panel (a). Parameters: $K = 0.5$, $T = 0.05$, $b = 1.025$.

size. Effects of the network structure have been studied in [24] and also in [10, 8], where motivated by a specific problem from neuroscience the dynamics of star shaped networks and tree networks have been studied.

In this paper, we come back to the original system of Shinomoto and Kuramoto [23]. We extend the approach of numerical bifurcation analysis for the thermodynamic limit from [21] by including also the dependence on the coupling strength and providing two-parameter continuations of the codimension-two points. In addition, we study in detail the noisy trajectories in finite size system in comparison to the dynamical scenarios obtained for the thermodynamic limit. While this has been done already in quite detail for specific parameter values in the regime of irregular collective spiking and collective oscillations [25], we are going also include the scenarios in the vicinity of the codimension two points. Moreover, we show how the characteristics of noisy trajectories in finite size system change with the system parameters within the different regions delineated in the two dimensional bifurcation diagram and in this way explain how the complex dynamics of the Fokker-Planck equation can be related to the stochastic properties of a finite size system.

The starting point is a nonlinear and nonlocal Fokker-Planck equation for the single particle distribution under the influence of a self-consistent global mean field. Using numerical bifurcation analysis for this equation of nonlocal semilinear parabolic type, one can obtain a complicated bifurcation diagram, which describes how the dynamical regimes in dependence of the main parameters of noise intensity and coupling strength are organized by a Takens-Bogdanov bifurcation combined with a cusp point and a fold-homoclinic point. Based on these results for the thermodynamic limit, we investigate the microscopic and collective behavior of finite size systems.

We consider a population of N identical active rotators

$$(1) \qquad \frac{d\theta_j}{dt} = 1 - b\sin\theta_j - \frac{K}{N}\sum_{k=1}^{N}\sin(\theta_j - \theta_k) + \sqrt{2T}\eta_j(t),$$

where $\theta_j \in \mathbb{S}^1 = \mathbb{R}/2\pi\mathbb{Z}$, $j = 1, \ldots, N$ are the phases and $\eta_j(t)$ are independent sources of white noise, satisfying $\langle\eta_j(t)\rangle = 0$, $\langle\eta_j(t)\cdot\eta_k(t')\rangle = \delta_{jk}\delta(t-t')$. The main parameters are the local excitability parameter b, the noise intensity T, and the strength K of the global attractive coupling. Throughout the paper, we fix the excitability parameter b to a value slightly above one, such that each unit is excitable with a stable fixed point at $\theta_0 = \arcsin 1/b$. Note that without coupling, i.e. $K = 0$, we have an ensemble of independent excitable units with noise. These noise sources from time to time cause excitations of individual units whose phases make revolutions. We call such events *individual spikes*, and since the noise sources are uncorrelated, the spiking of the uncoupled units is independent. On the other side, for vanishing noise $T = 0$ a positive coupling induces global stability of the homogeneous stable state $\theta_j(t) = \theta_0$. As we will see below, for strong enough coupling this homogeneous stable state behaves itself as a single excitable unit: if the noise of a certain level is added, it leads to the emergence of *collective spikes*, i.e. moments at which many units produce almost coincident spikes. For larger noise the irregular collective spiking transforms into periodic self-sustained collective oscillations, which can be interpreted as partially synchronized noise-induced oscillations of the individual oscillators.

2. Bifurcations in the thermodynamic limit

Let us first study the population dynamics in the thermodynamic limit $N \to \infty$. The joint probability density $\rho(\theta,t)$ for the units to be at time t in a neighborhood $[\theta, \theta + \delta\theta]$ evolves according to the Fokker-Planck equation

$$(2) \qquad \frac{\partial \rho(\theta,t)}{\partial t} = T\frac{\partial^2 \rho(\theta,t)}{\partial \theta^2} - \frac{\partial}{\partial \theta}\left[(1 - b\sin\theta - K\sigma)\rho(\theta,t)\right],$$

with periodic boundary conditions $\rho(\theta + 2\pi, t) = \rho(\theta,t)$ and the normalization condition $\int_{-\pi}^{\pi} d\theta \rho(\theta,t) = 1$. With

$$(3) \qquad \sigma = \int_{-\pi}^{\pi} d\theta' \sin(\theta - \theta')\rho(\theta',t)$$

we denoted the continuum version of the global coupling term in (1).

For our numerical bifurcation analysis we expand the 2π-periodic function $\rho(\theta,t)$ into a Fourier series

$$(4) \qquad \rho(\theta,t) = \frac{1}{2\pi}\sum_{n=-\infty}^{\infty} r_n(t)e^{in\theta},$$

where $r_n = r_{-n}^*$, since ρ is real, and $r_0 = 1$, due to normalization. Note that the complex Fourier coefficients

$$(5) \qquad r_n = \langle e^{-in\theta}\rangle = \int_{-\pi}^{\pi} d\theta e^{-in\theta}\rho(\theta,t),$$

concide with the complex Kuramoto-Daido order parameters and $R = |r_1|$ is the classical real Kuramoto order parameter. Then (2) transforms into a series of ODEs

$$(6) \qquad \frac{dr_n}{dt} = n\left\{\frac{K}{2}(r_1 r_{n-1} - r_{-1}r_{n+1}) + \frac{b}{2}(r_{n-1} - r_{n+1}) - (i + Tn)r_n\right\}, \qquad n \in \mathbb{N}.$$

Note that for a given trajectory $r_1(t)$ we can recover the microscopic dynamics of single oscillator by rewriting (1) as

$$(7) \qquad \frac{d\theta_j}{dt} = \omega - B(t)\sin(\theta_j + \psi(t)) + \eta_j(t),$$

where $B(t) = |b + Kr_1(t)|$ and $\psi(t) = \arg(b + Kr_1(t))$. In the case of an equilibrium state of (6) with a constant mean field r_1, the resulting constant B can be interpreted as the effective microscopic excitability parameter in the given regime.

Let us first determine the equilibrium states of (6). Equating the r.h.s. to zero, one obtains

$$(8) \qquad r_{n+1} = \frac{Kr_1 r_{n-1} + br_{n-1} - 2(i + Tn)r_n}{Kr_1^* + b},$$

which can be used for an iterative procedure to obtain a sequence $r_n \in \mathbb{C}, n > 1$ after choosing $r_1 \in \mathbb{C}$ (r_0 is always set equal to one). Because of the multiplication by n, the sequence diverges for the most of the choices of r_1, and only the values of r_1 leading to $r_n \to 0$ provide a converging Fourier series corresponding to equilibrium states of (6). Figure 1(a) illustrates the divergence of the coefficients by showing the number of iterations N after which r_n leaves the unit circle depending on initial choice $r_1 \in \mathbb{C}$ for some choice of the parameters. The sharp peaks show the locations of the equilibrium states.

At the equilibrium states, the order parameters r_n quickly converge to zero so that $\ln|r_n| \sim -n^2$ as demonstrated in Fig. 1(b). This allows us to truncate the infinite chain of equations (6). We have checked that for $T > 0.005$ and $K > 0.1$ and a truncation at $n = 30$ the remaining order parameters with $n > 30$ never exceed 10^{-3}. Note that for very small noise there may appear sharp peaks in the distributions $\rho(\theta)$ which can lead to a very slow convergence of the Fourier series such that an approximation of this type is no more adequate. However, for noise levels treated here we can stay with a system of thirty ODEs for complex variables. Further we consider this system as a proxy for system (2) and perform its systematic numerical bifurcation analysis using the MatCont toolbox [4].

For the bifurcation analysis shown in Figure 2 we fixed the excitability parameter $b = 1.025$ slightly above the threshold and use the coupling strength K and the noise intensity T as bifurcation parameters. The resulting bifurcation diagram is organized around three codimension-two points: a cusp point CP, a Bogdanov-Takens point BT, and a fold homoclinic point FH [13]. From the cusp point two curves of saddle-node bifurcations emerge. At the Bogdanov-Takens point, the lower saddle-node curve SN meets the Andronov-Hopf bifurcation curve AH and the saddle homoclinic bifurcation curve SH. The latter curve meets the upper saddle-node branch in the fold homoclinic point. Above this point, the saddle-node bifurcation becomes a saddle-node on invariant circle (SNIC).

In Fig. 3 we show how the cusp point and the Bogdanov-Takens point depend on the excitability parameter b. Note that both curves are confined to the region of b above the critical value $b = 1$. For b tending to one they occur at smaller noise T while also the corresponding values of the coupling strength decay to zero.
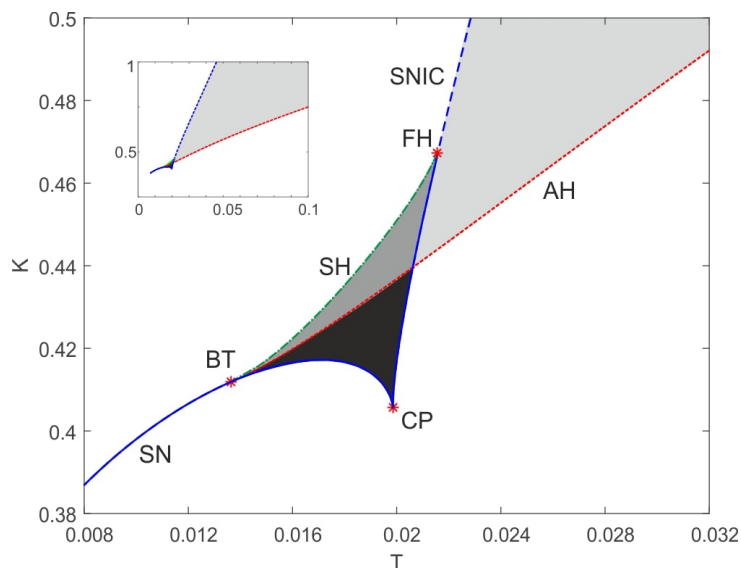
FIGURE 2. Bifurcation diagram of system (2) for fixed $b = 1.025$. CP – cusp point, BT – Bogdanov-Takens point, FH – fold-homoclinic point, SN – saddle-node curve (blue), SNIC – saddle-node on invariant circle (blue, dashed), AH – Andronov-Hopf curve (red, dashed), SH – saddle homoclinic curve (green, dot-dashed). Regions of different dynamical regimes: white – single stable steady state, light gray – collective oscillations, dark gray – coexistence of stable oscillations and a stable steady state, black – two coexisting stable steady states. The zoom out in the inset panel shows the locking cone in a larger parameter region.
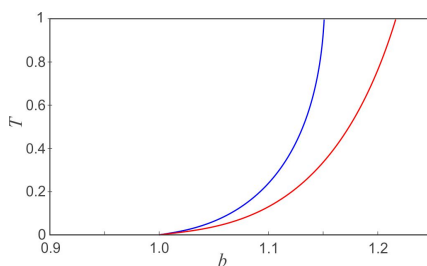

FIGURE 3. Curves of cusps (blue) and Bogdanov-Takens points (red) in the (b, T)-parameter plane

The codimension-two points for the Fokker-Planck equation (2) have been found by a similar numerical bifurcation analysis already in [21], however unfolded with the parameters T and b in a situation, where they occur at significantly larger noise levels. The main feature of the bifurcation scenario in the (T, K)-plane, shown in Figure 2, is the appearance of a cone-shaped region with stable collective oscillations. We will recall the main properties of these oscillations in Section 3, before we look in Section 4 at the more complicated region in the vicinity of the codimension-two points at the tip of the tilted locking cone, which also includes the regions of bistability.

3. COLLECTIVE OSCILLATIONS AND IRREGULAR COLLECTIVE SPIKING

The existence of collective oscillations and irregular collective spiking (sometimes called "collective firing"), induced by noise, diversity, or disorder in the coupling network has been reported already in Refs. [25, 26]. We will describe here in detail how the microscopic and macroscopic characteristics of these dynamical regimes depend on the parameters T and K. For larger values of the coupling strength K the tilted locking cone containing the stable collective oscillations is bounded to the left, i.e. for decreasing noise, by a SNIC bifurcation while for increasing noise it ends at a supercritical Andronov-Hopf bifurcation, see Fig. 2. Crossing the locking cone by varying the noise level at a fixed coupling strength K above the FH point, we observe a sequence of characteristic changes of the dynamics. At a noise level short below the SNIC, we observe a regime of irregular collective spiking. The reason for this is that in this region, the stable stationary solution of the Fokker-Planck equation (2), is excitable. Indeed, the closeness to the SNIC leads to the fact that for sufficiently strong perturbations the Fokker-Planck equation responds with a large excursion along the invariant circle (red curve in Fig 4(a)), corresponding to a collective spike. In finite size systems the spikes are triggered by the mean field noise, which
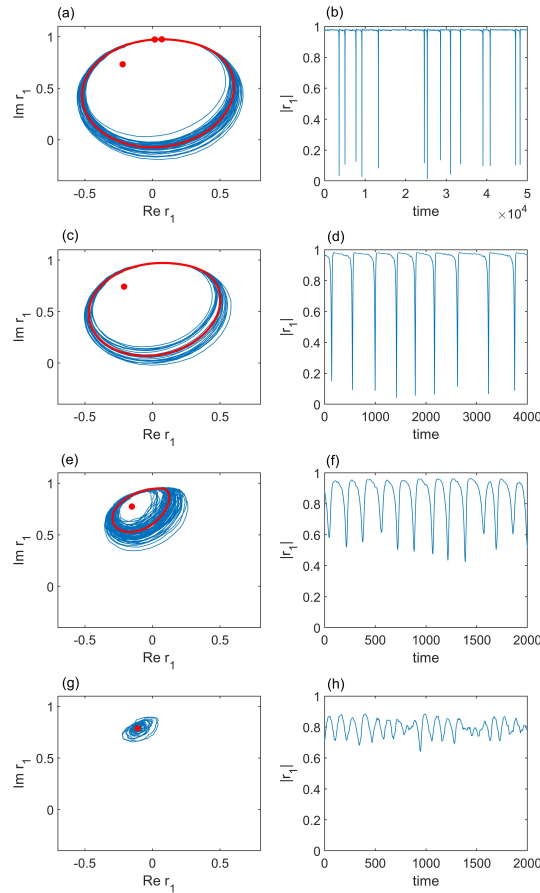
FIGURE 4. Phase portraits (left column) and time traces (right column) of the order parameter $R = |r_1|$ for system (1) (blue) with $N = 2000$ and for the Fokker-Planck equation (2) (red) at $K = 0.6$ and different choices of the noise intensity. (a), (b) – irregular collective spiking at $T = 0.0267$; (c), (d) – collective oscillations at $T = 0.03$; (e), (f) – small amplitude collective oscillations at $T = 0.045$; (g), (h) – noise-induced small amplitude oscillations after the Andronov-Hopf bifurcation at $T = 0.6$.

results from the addition of the individual noise sources and scales as $\sqrt{2T/N}$ (for details see, [25]). Hence, the rate of the resulting irregular collective spiking depends not only on the distance to the SNIC, but also on the system size. The collective oscillations within the locking cone show for increasing noise a decreasing amplitude in the mean field, which can be explained as a result of decreasing coherence among the oscillators. At the same time the collective frequency increases. After the Andronov-Hopf bifurcation we reach a stable equilibrium. Fig. 4 shows corresponding phase portraits and time traces of the order parameter for system (1) with $N = 2000$ together with the corresponding phase portraits for the Fokker-Planck equation (2). For the numerical simulation of system (1) we used the Euler-Maruyama method with the fixed time step $\delta t = 0.002$, while the trajectories of the Fokker-Planck equation (2) were obtained by integration of system (6) truncated at $n = 30$.

In Fig. 5 we show how several characteristic quantities vary along the branches of stationary and periodic solutions of (2) for varying the noise intensity T in a cross-section through the locking cone at $K = 0.6$. In panel (a) we show the global Kuramoto order parameter R. Note that the branch of collective oscillations mediates a transition between two branches of stable equilibria. The substantial decrease of the order parameter during this transition is reflected by reduced microscopic excitability parameter B, shown in panel (b), which, however, remains still bigger than the microscopic excitability $b = 1.025$ of the uncoupled units. In panels (a) and (b) we display also the time averages $\langle R \rangle$ and $\langle B \rangle$ along noisy trajectories of (1) with $N = 2000$. Here and further, we used the time interval $\Delta t = 10^5$ for the averaging. For finite size systems, we observe fluctuations in the order parameter, which again depend not only on the noise level, but also on the system size.
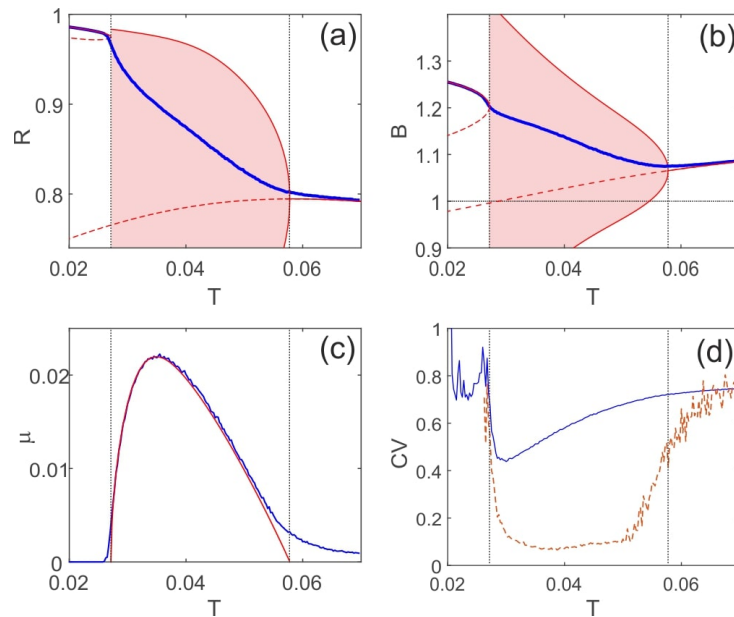
FIGURE 5. Cross-sections through the locking cone (vertical dashed lines) at $K = 0.6$ and varying T. Panel (a): red curves – order parameter R along branches of stationary and periodic solutions of the Fokker-Planck equation (2), solid/dashed – stable/unstable branches, shaded region – range of $R(t)$ for periodic solutions, blue curve – time average $\langle R(t) \rangle$ for system (1) with $N = 2000$. Panel (b): effective microscopic excitability parameter B and time average $\langle B(t) \rangle$ (coloring as in (a)). Panel (c): blue curve – variance μ of order parameter $R(t)$ for system (2) with $N = 2000$, red curve – corresponding value along periodic orbit of (2). Panel (d): coefficient of variation for individual (blue) and collective (red) inter-spike intervals for system (2) with $N = 2000$.

We characterize theses macroscopic fluctuations by the variability of the Kuramoto order parameter

$$(9) \qquad \mu = \langle (R - \langle R \rangle)^2 \rangle,$$

where $\langle \cdot \rangle$ denotes time averaging. Note however, that this quantity is nonzero inside the locking cone even in the thermodynamic limit. Fig. 5(c) shows that the macroscopic variability strongly increases before the SNIC, indicating the collective excitability, and decreases for increasing noise after the Andronov-Hopf bifurcation, indicating how increasing the noise level beyond the resonance actually increases the collective order.

In the oscillatory regime the mean frequency of the individual noise-induced spikes is always higher than the collective frequency. This means that there are also individual spikes that do not contribute to a collective oscillation. In terms of the Fokker-Planck equation, there is a permanent positive flux through the rotating peak of the collective oscillation. Fig. 6(a) shows the distribution of the inter-spike intervals of individual units for $K = 0.6$ and different values of T, obtained from the effective single unit equation (7), driven by the periodic regime of the thermodynamic limit (2). In order to obtain these distributions, we integrated Eq. (7) for the time interval $\Delta t \geq 10^8$ and recorded the timing of the spikes. The spike time is the moment when the phase crosses the level $\theta = \pi$. For each simulation, we obtained $\geq 10^6$ spikes. In the oscillatory regime, we observe multiple peaks, where the highest frequency peak corresponds to the not contributing spikes while the other peaks correspond to the collective frequency and its multiples.

For the finite size system this effect is also present, but the collective spikes are less regular and hence there is a broadening of the corresponding peaks in the distributions of the individual inter-spike intervals. Figures 6(b), (c) demonstrate the distributions of the individual and collective inter-spike intervals obtained for $N = 2000$ and two different noise levels. In order to obtain these distributions, the system was integrated for $\Delta t \geq 5 \times 10^4$, and the timing of the individual and collective spikes was recorded. The collective spike time is the moment when the order parameter crosses the level $R = 0.8$ downwards. For each simulation, we obtained ≥ 2000 collective and $\geq 5 \times 10^5$ individual spikes.

The corresponding coefficients of variation for individual and collective inter-spike intervals are shown in Fig. 5(d). One can see that the variability is substantially reduced in the oscillatory regime, where both quantities go through a minimum for increasing noise. The minimal variability of the individual inter-spike intervals is reached almost immediately after the onset of collective oscillations at the SNIC, while the most regular collective motion can be observed around the middle of
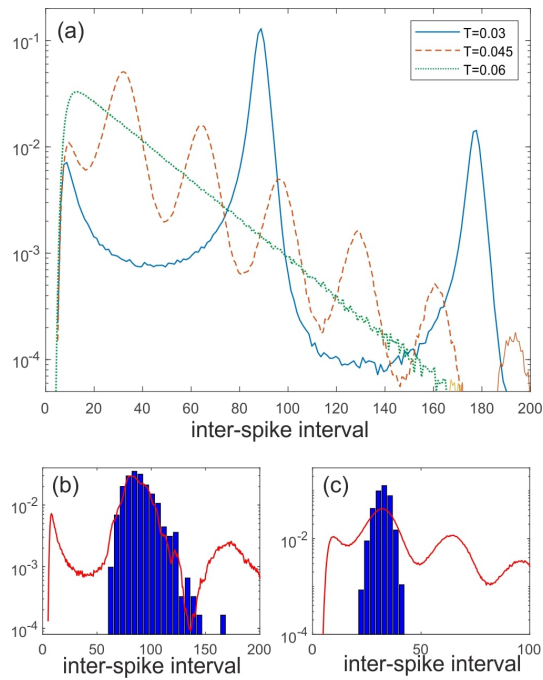
FIGURE 6. (a) Distributions of the inter-spike intervals of individual units from (7) for $K = 0.6$ and different values of T (indicated in the panels). (b), (c) Distributions of individual (red) and collective (blue) inter-spike intervals from system (1) (blue) with $N = 2000$ and (b) $K = 0.6$, $T = 0.03$, (c) $K = 0.6$, $T = 0.045$.

the locking cone. This leads to the counterintuitive observation that the superposition of less regular individual spike trains can result in a more regular collective oscillation.

4. SWITCHING, BURSTING AND AMPLITUDE VARIABILITY

The bifurcation diagram in Figure 2 shows that there is a region of particular complexity around the tip of the locking cone, organized by three codimension-two bifurcations of the Fokker-Planck equation (2). In this region the dynamics of (2) can be characterized by the qualitatively different planar flows being present in the normal forms of the respective codimension-two bifurcations in their two-dimensional center manifolds. For finite systems (2), one has to consider the impact of the finite size fluctuations on these deterministic dynamics of the thermodynamic limit. Figure 7 shows three specific examples of such qualitatively different regimes of the Fokker-Planck equation together with noisy trajectories from simulations of a finite size system with $N = 2000$, which will be discussed in detail within this Section.

At the cusp point emerges a region of bistability for coupling strengths above the cusp. This can be understood as follows: for coupling strengths below this critical value an increasing noise just leads to a higher individual spiking rate. Together with the coupling this induces a decreasing effective microscopic excitability parameter B, which in turn increases the spiking rate as well. This self-reinforcing process leads to the folding of the branch and the coexistence of two stationary states with different levels of the order parameter R, the excitability parameter B and the resulting spiking rate. This phenomenon can be observed already for a single noisy excitable unit with a feedback mechanism [9, 5] and also in a globally pulse-coupled system of such units [16]. In the latter, however, the coupling acts only as an activating, but not as a synchronizing force, such that the most of the other effects discussed here are not present. The resulting bistability in the Fokker-Planck equation corresponds for finite size systems to a regime of stochastic switching between metastable states. This switching process of Eyring-Kramers type is driven, similar as the irregular collective spikes, by the mean field noise such that the switching times also depend on the system size.

In Fig. 8 we show the order parameter R (panel (a)), the excitability parameter B (panel (b)) along the branches of stationary solutions of (2) for varying the noise intensity T in a cross-section through the bistability region at $K = 0.415$, directly above the cusp. For the finite size system, we calculated the time averages of these quantities over the time interval $\Delta t = 10^5$ which show a transition between the two branches of stable equilibria. This gradual transition is caused by gradually changing switching rates of the Eyring-Kramers process. Indeed, close to fold the switches to the metastable state on the folded branch occur at a much lower rate than the switches back to the other metastable state. Crossing the bistability
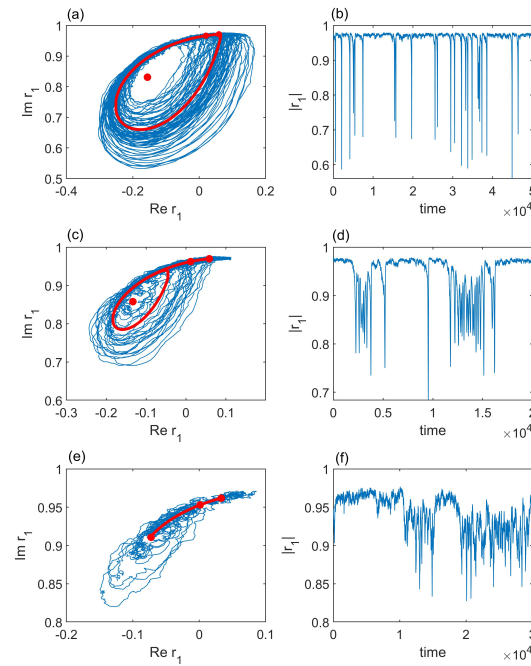
FIGURE 7. Phase portraits (left column) and time traces (right column) of the order parameter for system (1) (blue) with $N = 2000$ and for the Fokker-Planck equation (2) (red) for different dynamical regimes in the vicinity of the codimension-two points: (a), (b) – regime of irregular collective spiking close to fold homoclinic at $K = 0.475, T = 0.0215$, showing the amplitude variability of the collective spikes. (c), (d) – coexistence of a limit cycle and a fixed point at $K = 0.45, T = 0.02075$, leading to stochastic bursting. (e), (f) – coexistence of two stable fixed points at $K = 0.415, T = 0.0199$ leading to stochastic switching.

region the two metastable states interchange their role such that there is an intermediate regime of balanced switching, where switches in both directions occur at equal rate.

Figure 8(d) shows the distribution of $\arg r_1$ for the fixed noise level inside the bistability region (since the absolute values of r_1 in both stable states are close to each other, we chose to show the argument of r_1 instead). The bimodal distribution of the order parameter is a clear indication for the fluctuation-induced switching dynamics between the two metastable states of the Fokker-Planck equation. Note that the state with the lower order parameter R shows much larger fluctuations than the state with the higher order parameter , see Fig. 7(e), (f). Hence, the overall variability μ of the order parameter, shown in Fig. 8(c) has to be interpreted as an average over the different levels of local fluctuations around the two metastable states plus the variability induced by the switching. Note that also this collective temporal disorder decreases for increasing noise level beyond the region of bistability.

In contrast to the pulse coupled system studied in Ref. [16], an increasing coupling strength induces here a synchronization of the individual spiking, but only for the state with higher spiking rate. In this way, the onset of collective synchronization at the Andronov-Hopf bifurcation of the high activity state leads to the regime of coexistence of a stable collective oscillation with the stationary state of incoherent low activity. The influence of noise on systems with a coexistence of a stable limit cycle and a stable equilibrium has already been studied in [29]. For the state shown in Fig. 7(c), (d), the distributions of individual and collective inter-spike intervals are given in Fig. 9(a). The coefficient of variation of the collective inter-spike intervals (the so-called Fano factor) equals 1.58, which underlines that this state has the characteristics of stochastic bursting.

For the state shown in Fig. 7(a), (b) we have chosen the parameters $K = 0.475, T = 0.0215$ in the vicinity of the fold-homoclinic bifurcation. For the finite size system we observe in this region a gradual transition from the regime of collective excitability, induced by the SNIC, to the stochastic bursting described above. The intermediate regime is characterized by a highly irregular collective spiking, which due to the complex two-dimensional nonlinear dynamics in the Fokker-Planck equation also shows large fluctuations in the amplitude of the collective spikes. These amplitude fluctuations turn out to be significantly correlated with the fluctuations of the collective inter-spike intervals, the correlation coefficient being as
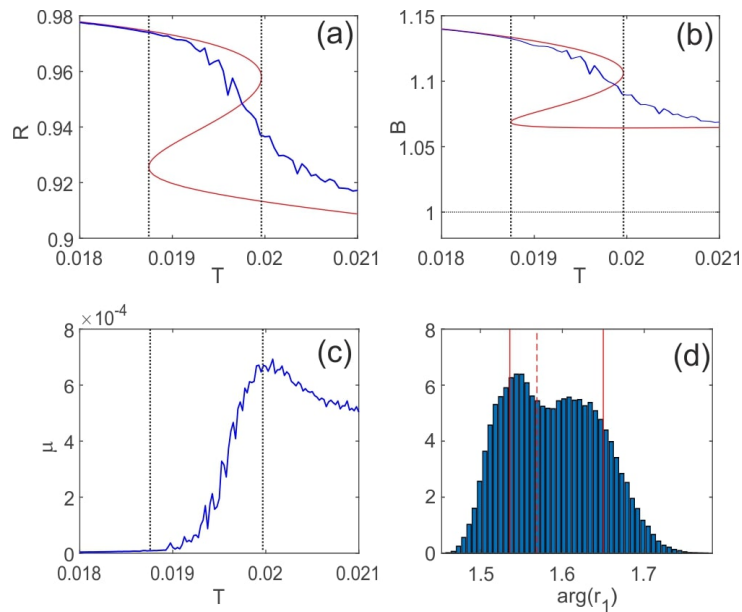
FIGURE 8. Cross-sections through the bistable region (indicated by vertical dotted lines in (a)–(c)) at $K = 0.415$ and varying T. Panel (a): red curves – order parameter R along branches of stationary solutions of the Fokker-Planck equation (2), solid/dashed – stable/unstable branches, blue curve – time average $\langle R(t) \rangle$ for system (1) with $N = 2000$. Panel (b): effective microscopic excitability parameter B and its time average $\langle B(t) \rangle$ (coloring as in (a)). Panel (c): variance μ of order parameter $R(t)$ for system (1) with $N = 2000$. Panel (d): distribution of $\arg(r_1)$ for system (1) with $N = 2000$ in the bistable regime at $K = 0.415, T = 0.0199$. Red lines – positions of stable (solid) and unstable (dashed) stationary solutions of (2).
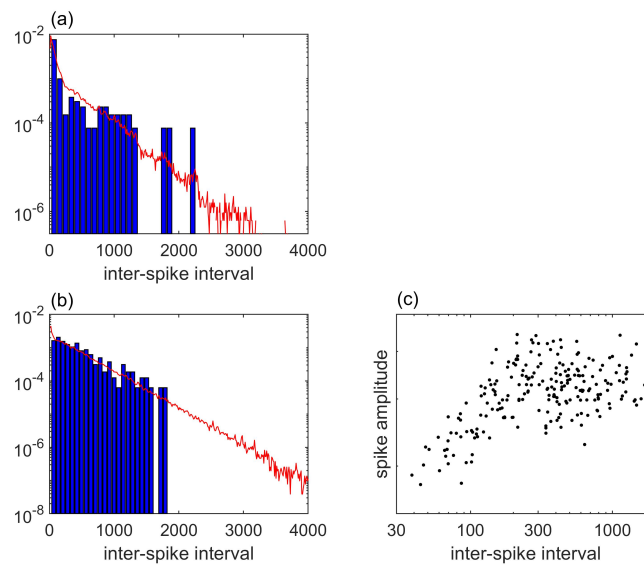

FIGURE 9. (a) Distributions of inter-spike intervals in the regime of stochastic bursting ($K = 0.45, T = 0.02075$). (b), (c) Excitable regime close to the FH-point ($K = 0.475, T = 0.0215$). (b) Distributions of individual (red) and collective (blue) inter-spike intervals from system (1) with $N = 2000$. (c) Correlation between amplitudes and successive inter-spike intervals of collective spikes (note the logarithmic scale of the horizontal axis).
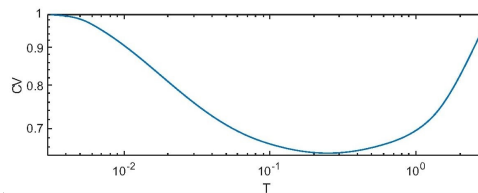
FIGURE 10. Coherence resonance of a single excitable unit for $b = 1.025$: the coefficient of variation of the inter-spike intervals versus the noise level.

large as $r \approx 0.3$. This correlation can also be seen from Fig. 9(c) where the time interval to the *successive* collective spike is plotted versus the amplitude of the *current* spike. Indeed after a small amplitude spike, there is a significantly increased probability for a subsequent short inter-spike interval, which leads to an extremely broad distribution of the inter-spike intervals, see Fig. 9(b). This indicates that in the vicinity of the tip of the locking cone, the collective dynamics is characterized by a maximum in the variability, which decreases not only for deviations in the noise level, but also in the coupling strength.

5. CONCLUSION AND OUTLOOK

In systems of excitable units driven by individual noise and coupled by an attractive mean-field coupling one can observe a huge variety of noise-induced dynamical effects with a complicated interplay of individual and collective order. We extended previous research on such systems by combining a bifurcation analysis of the Fokker Planck equation for the thermodynamic limit with a detailed analysis of the dynamics of noisy trajectories in finite size systems. We provided a bifurcation diagram in the parameter plane of noise intensity versus coupling strength, where collective oscillations can be found in a cone-shaped region with several specific properties:

- The locking cone is tilted (cf, Fig. 2). This can be explained by the fact that higher coupling strength also stabilizes the resting state of the individual oscillators such that a higher amount of noise is necessary to induce oscillations.
- At the side of lower noise, the locking cone is delineated by a SNIC bifurcation, where the collective oscillations disappear with zero frequency, which is related to the decreasing frequency of the individual noise-induced spikes.
- At the side of higher noise, the locking cone is delineated by an Andronov-Hopf bifurcation, where the collective oscillations are blotted out by the increasing noise.
- The tip of the locking cone is located at a specific coupling strength and noise level and the dynamics in the vicinity of this region are governed by a complicated bifurcation scenario, which can be obtained from the Fokker-Planck equation for the thermodynamic limit. In systems of finite size, this region is also characterized by the fact that the fluctuations of the individual noise sources induce a high variability in the collective behavior.

In contrast to earlier studies we provided also a detailed analysis of the dynamical regimes close to the tip of the locking cone and characterized the corresponding effects in finite size systems. We demonstrated regimes with stochastic switching, fluctuation induced bursting, and amplitude variability of irregular spiking. Studying the noise dependence of the variability of collective and individual inter-spike intervals, we pointed out that both depend in a non-monotonous way on the noise level and the superposition of less regular individual spike trains can indeed result in a more regular collective oscillation.

Our study also reveals that the relation between noise-induced oscillations in individual units and the population of coupled units is highly nontrivial and cannot be explained as a straight forward synchronization of noise induced oscillations at coherence resonance, i.e. at the noise level where the individual noise-induced spikes are most regular with a specific frequency. As shown in Fig. 10, for the parameter values used in the present paper, the coherent resonance takes place at $T \approx 0.25$. One could expect that at this very noise level an attractive mean-field coupling of such units would lead most easily to a synchronization of the individual noise-induced oscillations. In our example of excitable phase oscillators with Kuramoto type coupling, we observe the onset of collective oscillations at a much lower noise level and with a frequency close to zero. At the same the time effective excitability parameter in the disordered state of the coupled system differs substantially from the corresponding parameter for the uncoupled units. Hence, it might be that different coupling mechanisms could lead to qualitatively different scenarios.

REFERENCES

[1] V. S. Anishchenko, V. Astakhov, A. Neiman, T. Vadivasova, and L. Schimansky-Geier. Nonlinear Dynamics of Chaotic and Stochastic Systems: Tutorial and Modern Developments (Springer Series in Synergetics). Springer-Verlag, Berlin, Heidelberg, 2007.

[2] T. M. Antonsen, R. T. Faghih, M. Girvan, E. Ott, and J. Platig. External periodic driving of large systems of globally coupled phase oscillators. Chaos: An Interdisciplinary Journal of Nonlinear Science, 18(3):037112, 2008.

[3] L. M. Childs and S. H. Strogatz. Stability diagram for the forced kuramoto model. Chaos: An Interdisciplinary Journal of Nonlinear Science, 18(4):043128, 2008.

[4] A. Dhooge, W. Govaerts, Y. A. Kuznetsov, H. G. E. Meijer, and B. Sautois. New features of the software matcont for bifurcation analysis of dynamical systems. Mathematical and Computer Modelling of Dynamical Systems, 14:147–175, 2008.

[5] I. Franović, S. Yanchuk, S. Eydam, I. Bačić, and M. Wolfrum. Dynamics of a stochastic excitable system with slowly adapting feedback. Chaos: An Interdisciplinary Journal of Nonlinear Science, 30(8):083109, 2020.

[6] V. Klinshov and I. Franović. Two scenarios for the onset and suppression of collective oscillations in heterogeneous populations of active rotators. Physical Review E, 100(6):62211, 2019.

[7] V. V. Klinshov, D. A. Zlobin, B. S. Maryshev, and D. S. Goldobin. Effect of noise on the collective dynamics of a heterogeneous population of active rotators. Chaos: An Interdisciplinary Journal of Nonlinear Science, 31(4):043101, 2021.

[8] J. Kromer, A. Khaledi-Nasab, L. Schimansky-Geier, and A. B. Neiman. Emergent stochastic oscillations and signal detection in tree networks of excitable elements. Scientific Reports, 7(1):3956, 2017.

[9] J. A. Kromer, R. D. Pinto, B. Lindner, and L. Schimansky-Geier. Noise-controlled bistability in an excitable system with positive feedback. EPL (Europhysics Letters), 108(2):20007, oct 2014.

[10] J. A. Kromer, L. Schimansky-Geier, and A. B. Neiman. Emergence and coherence of oscillations in star networks of stochastic excitable elements. Phys. Rev. E, 93:042406, 2016.

[11] Y. Kuramoto. Chemical Oscillations, Waves, and Turbulence. Dover Books on Chemistry Series. Dover Publications, 2003.

[12] L. Lafuerza, P. Colet, and R. Toral. Nonuniversal results induced by diversity distribution in coupled excitable systems. Physical Review Letters, 105(8):084101, 2010.

[13] P. S. Leonid, L. S. Andrey, V. T. Dmitry, and O. C. Leon. Methods of qualitative theory in nonlinear dynamics. Part II. World Scientific, 2001.

[14] B. Lindner, J. García-Ojalvo, A. Neiman, and L. Schimansky-Geier. Effects of noise in excitable systems. Physics Reports, 392(6):321–424, 2004.

[15] A. Neimann, A. Silchenko, V. Anishchenko, and L. Schimansky-Geier. Stochastic resonance: Noise-enhanced phase coherence. Physical Review E, 58(6):7118–7125, 1998.

[16] K. P. O'Keeffe and S. H. Strogatz. Dynamics of a population of oscillatory and excitable elements. Physical Review E, 93(6):62203, 2016.

[17] E. Ott and T. M. Antonsen. Low dimensional behavior of large systems of globally coupled oscillators. Chaos: An Interdisciplinary Journal of Nonlinear Science, 18(3):37113, 2008.

[18] E. Ott and T. M. Antonsen. Long time evolution of phase oscillator systems. Chaos: An Interdisciplinary Journal of Nonlinear Science, 19(2):23117, 2009.

[19] A. Pikovsky, M. G. Rosenblum, and J. Kurths. Synchronization, A Universal Concept in Nonlinear Sciences. Cambridge University Press, Cambridge, 2001.

[20] A. S. Pikovsky and J. Kurths. Coherence resonance in a noise-driven excitable system. Phys. Rev. Lett., 78:775–778, Feb 1997.

[21] H. Sakaguchi, S. Shinomoto, and Y. Kuramoto. Phase transitions and their bifurcation analysis in a large population of active rotators with mean-field coupling. Progress of Theoretical Physics, 79(3):600–607, 1988.

[22] N. Semenova, A. Zakharova, V. Anishchenko, and E. Schöll. Coherence-resonance chimeras in a network of excitable elements. Phys. Rev. Lett., 117:014102, Jul 2016.

[23] S. Shinomoto and Y. Kuramoto. Phase Transitions in Active Rotator Systems. Progress of Theoretical Physics, 75:1105, 1986.

[24] B. Sonnenschein, M. Zaks, A. Neiman, and L. Schimansky-Geier. Excitable elements controlled by noise and network structure. Eur. Phys. J. Spec. Top., 222:2517—-2529, 2013.

[25] C. J. Tessone, A. Scire, R. Toral, and P. Colet. Theory of collective firing induced by noise or diversity in excitable media. Physical Review E, 75(1):16203, 2007.

[26] C. J. Tessone, D. H. Zanette, and R. Toral. Global firing induced by network disorder in ensembles of active rotators. The European Physical Journal B, 62(3):319–326, 2008.

[27] R. Toral, C. R. Mirasso, and J. D. Gunton. System size coherence resonance. Europhysics Letters, 61(2):162—-167, 2003.

[28] N. Wiener and A. Rosenblueth. The mathematical formulation of the problem of conduction of impulses in a network of connected excitable elements, specifically in cardiac muscle. Arch. Inst. Cardiol. Mex., 16(3):205–65, 1946.

[29] A. Zakharova, T. Vadivasova, V. Anishchenko, A. Koseska, and J. Kurths. Stochastic bifurcations and coherencelike resonance in a self-sustained bistable noisy oscillator. Phys. Rev. E, 81:011106, Jan 2010.

[30] M. A. Zaks, A. B. Neiman, S. Feistel, and L. Schimansky-Geier. Noise-controlled oscillations and their bifurcations in coupled phase oscillators. Physical Review E, 68(6):66206, 2003.